SUPPORTING INFORMATION

Anti-amyloidogenic amphipathic arginine-dehydrophenylalanine spheres capped selenium nanoparticles as potent therapeutic moieties for Alzheimer's disease

Avneet Kour[a,b], Virendra Tiwari [c], Nidhi Aggarwal[a], Himanshu Sekhar Panda[a], Ashwani Kumar[b] ,Siddharth Tiwari[d], V. S. Chauhan[e], Shubha Shukla[c*], Jiban Jyoti Panda[a*]

[a]Institute of Nano Science and Technology, Mohali, Punjab 140306, India

[b] University Institute of Pharmaceutical Sciences, Punjab University, Chandigarh 160014, India

[c] CSIR-Central Drug Research Institute, Sector 10, Jankipuram Extension, Sitapur Road, Lucknow 226031, India

[d] National Agri-food Biotechnology Institute (NABI), Mohali, Punjab 140308, India

[e] International Centre for Genetic Engineering and Biotechnology, New Delhi 110067, India

Corresponding author

*Email:shubha_shukla@cdri.res.in, Shubha Shukla

*Email: jyoti@inst.ac.in, Jiban Jyoti Panda

Information S1. Synthesis of Ac-PHF6

Fmoc-Rink Amide MBHA resin was swollen utilizing dimethylformamide (DMF) for 0.5 hour (h). Microwave-assisted Fmoc deprotection was achieved utilizing 20% piperazine in DMF. Each Fmoc-amino acid coupling step was carried out with microwave heating using di-isopropyl carbodiimide (DIC) as an activator and oxyma as a base in DMF. 20% acetic anhydride in DMF was used for achieving final acetylation of the N-terminus. The resin was filtered, washed with dichloromethane (DCM) and further allowed to air dry. The peptides were subjected to cleavage from the resin utilizing a mixture of trifluoroacetic acid/thioanisole/1,2- ethanedithiol/anisole (90: 5: 3: 2, v/v/v/v) for 3 h at RT. The cleaved peptide-TFA solution was filtered and further

precipitated by drop-wise addition of ice cold (-20°C) diethyl ether. The product precipitated, was centrifuged for 10 minutes (min) at 7000 rpm and afterwards the pellet was washed thrice with chilled diethyl ether and vacuum dried. The dried peptide was dispersed in a mixture of acetonitrile/H_2O containing 0.1% TFA and purified through RP-HPLC (Waters HPLC system) with a C18- column with an acetonitrile-water gradient containing 0.1% trifluoroacetic acid. HPLC chromatograms of purified peptides were obtained. Molecular weights were confirmed by ESI-MS recorded by Waters, Q-TOF Micromass instrument.

Information S2: Synthesis of the dipeptide, arginine-α, β-dehydro phenylalanine (RΔF)

The synthesis of the dipeptide, arginine-α, β-dehydro-phenylalanine (RΔF) was carried out utilizing standard solution-phase peptide synthesis methods.[1,2]The synthesized peptide was further purified using HPLC and analyzed using mass spectrometry.

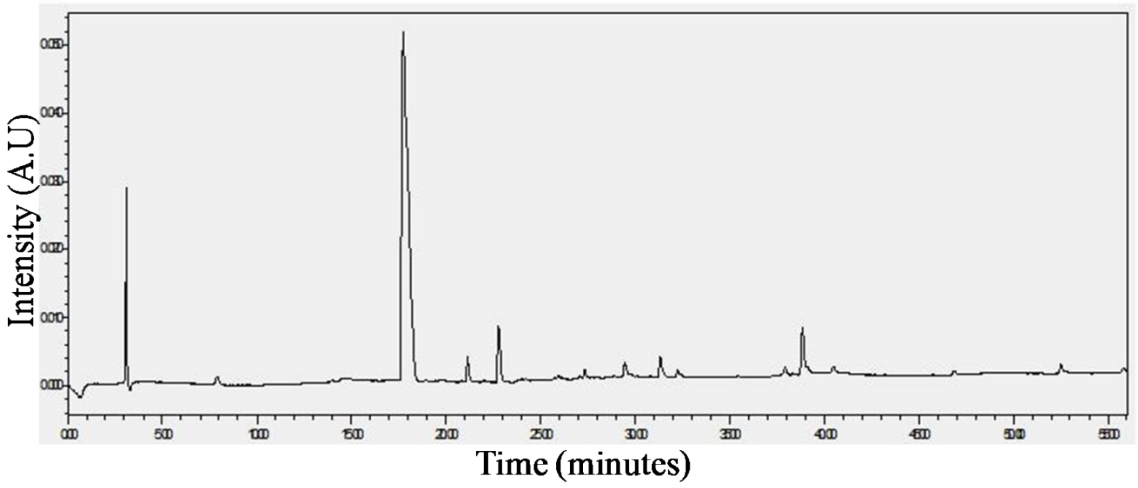

Figure S1A. HPLC profile of RΔF

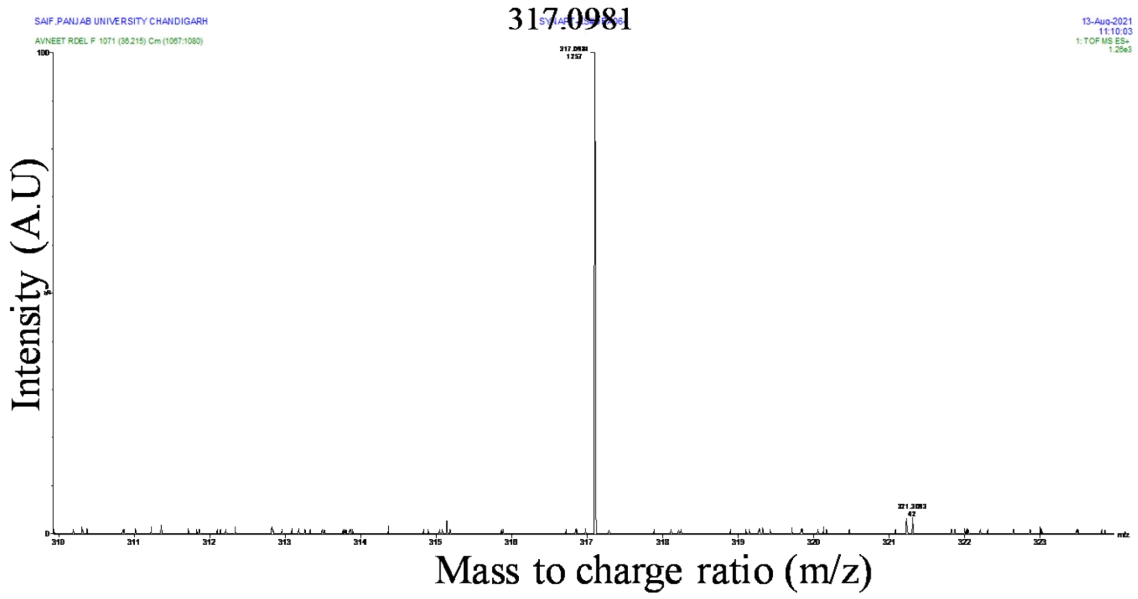

Figure S1B. Mass spectrometric profile of RΔF, (Observed mass: 317.09 Da and expected mass: 317 Da)

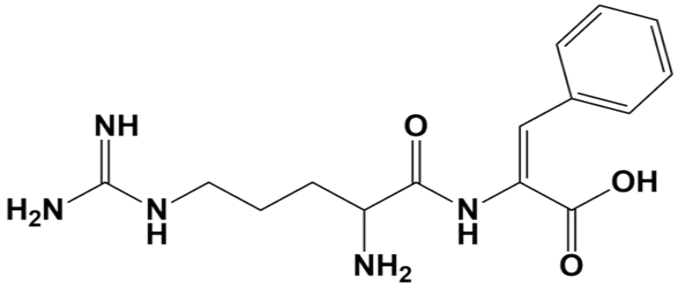

Figure S2. Chemical structure of RΔF

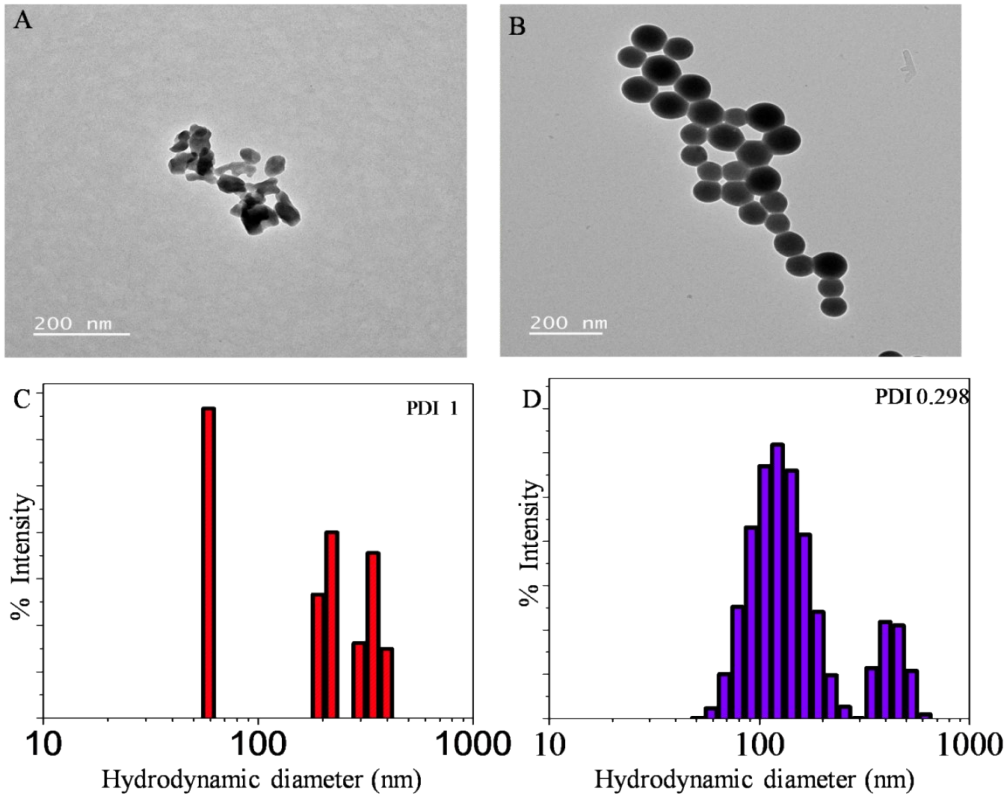

Figure S3. TEM images of (A) SeNPs and (B) RΔF NPs (Scale bar is 200 nm). Hydrodynamic size of (C) SeNPs and (D) RΔF NPs

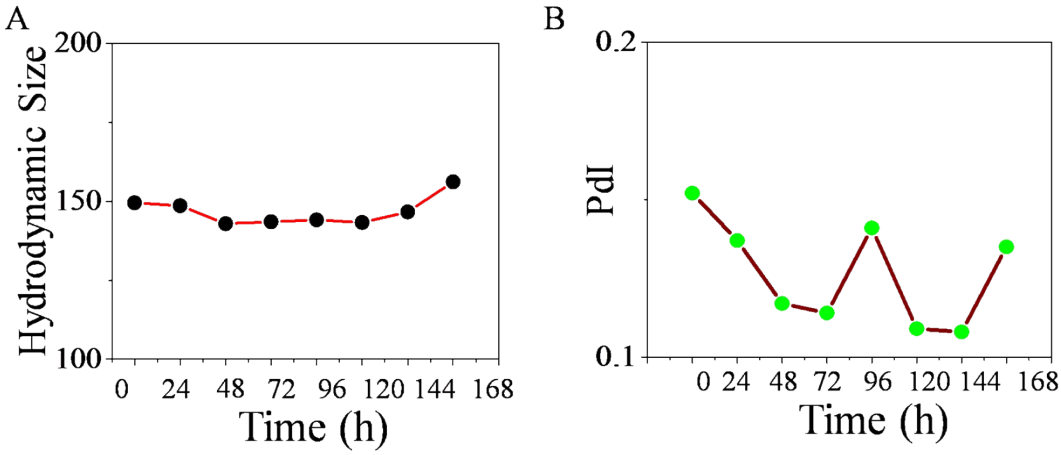

Figure S4. Stability of RΔF-SeNPs determined for a period of 168 h. (A) Change in hydrodynamic size of the particles over a period of 168 h (B) Change in polydispersity index (PDI) of RΔF-SeNPs over a period of 168 h (7 days) in DMEM/F12 media containing 10% FBS. No variation in the size and polydispersity index of the particles was observed till 168 h (7 days).

Information S3. Synthesis of diphenylalanine (FF)

Synthesis of FF was done using solution phase peptide synthesis methods as described earlier in

our previous report.[3,4] The synthesized dipeptide was purified using a C18 column running on a linear gradient of 5-95% of acetonitrile to water and was analyzed by mass spectrometry (Waters Q-TOF Micromа (Q-TOF) as reported earlier.[3]

Information S4. Synthesis of AcPHF6 (Ac-VQIVYK-NH_2)

Mass spectrum showed the expected mass (790 Da) for AcPHF6 (Ac-VQIVYK-NH_2) (Figure S5).

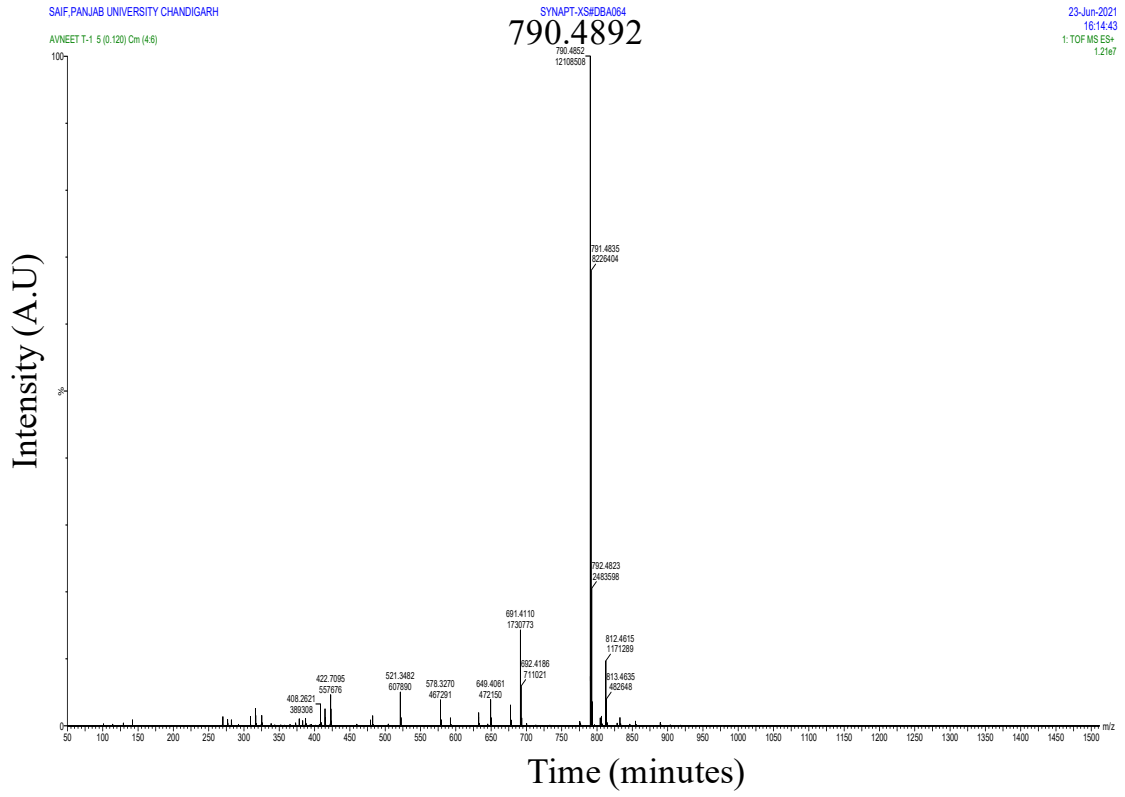

Figure S5. Mass spectrometric profile of the hexapeptide, Ac-PHF6 (Ac-VQIVYK-NH_2). (Observed mass 790.4892 Da; expected mass 790 Da)

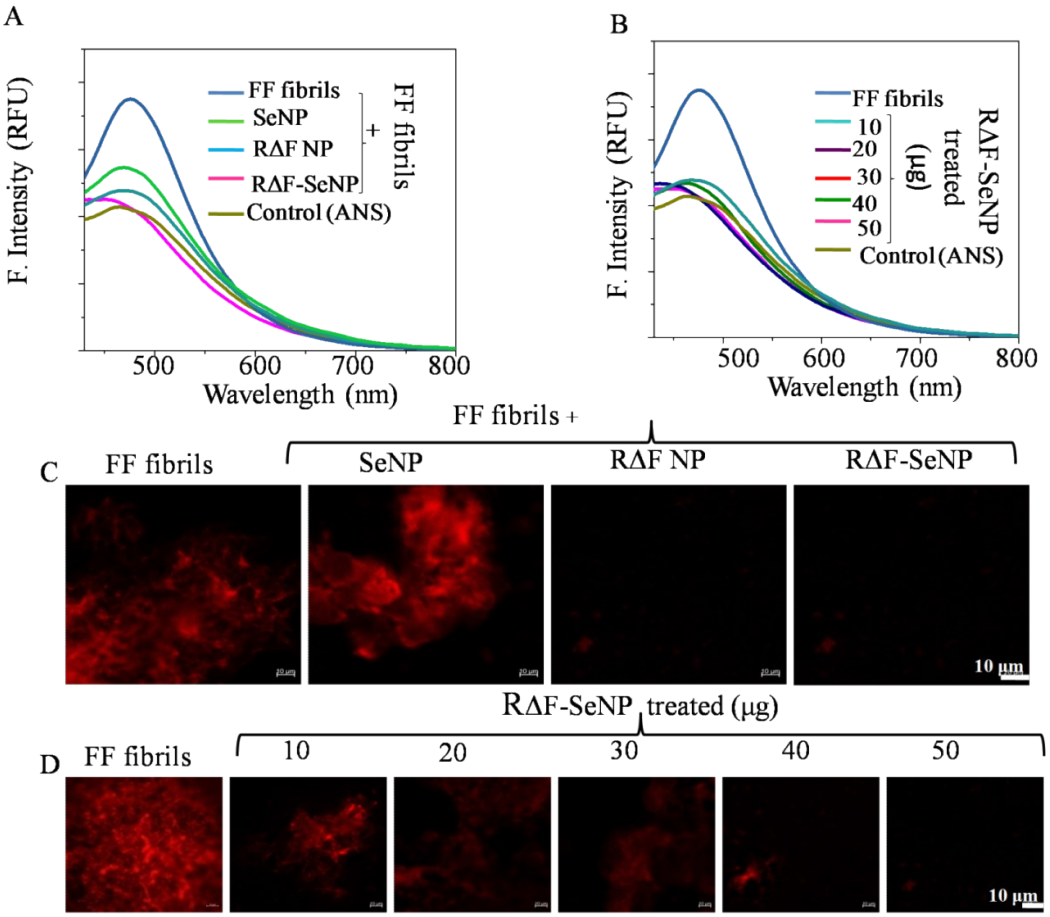

Figure S6 (A) Assessment of Bis-ANS fluorescence spectra of FF fibrils co-incubated with SeNP, RΔF NP, RΔF-SeNP. (B) Bis ANS assay of FF fibrils co-incubated with different concentrations of RΔF-SeNPs. These results showed a decline in the fluorescence intensity of the fibrils with an increase in the concentration of the RΔF-SeNPs. (C) Confocal images of Bis-ANS stained FF fibrils incubated with SeNP, RΔF NP, and RΔF-SeNPs. Microscopic analysis revealed a loss in the red fluorescence signal when fibrils were co-incubated with RΔF-SeNPs. (D) Concentration-dependent decline in the Bis-ANS fluorescence intensity when FF fibrils were co incubated with different concentrations of RΔF-SeNPs. These results were in alignment with our SEM and ThT analysis results pertaining to the fibril dissociating nature of the NPs.

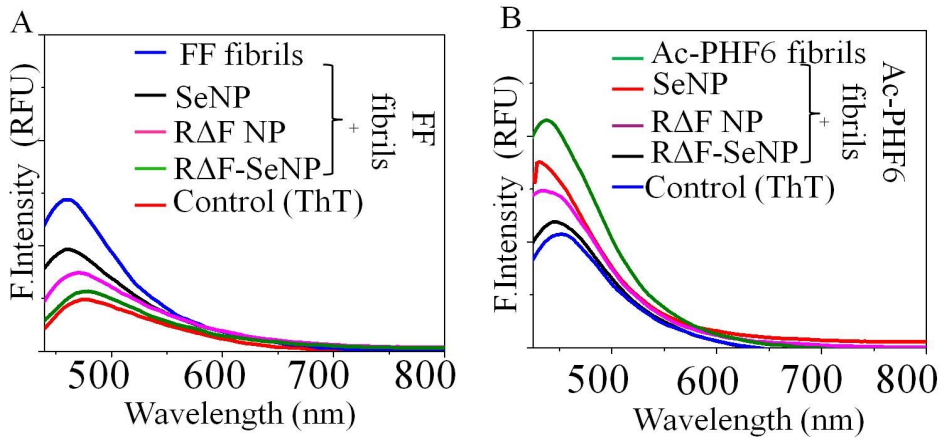

Figure S7. (A) ThT fluorescence assay of NPs incubated with FF after the initiation of the fibrillization process. Results showed the inhibitory potency of the NPs toward the initiation of the aggregation process of FF. (B) Similarly, ThT fluorescence assessment of NPs incubated with Ac-PHF6 fibers. Results depicted inhibition of the initiation of fibrillization process of Ac-PHF6 peptide after treatment with NPs.

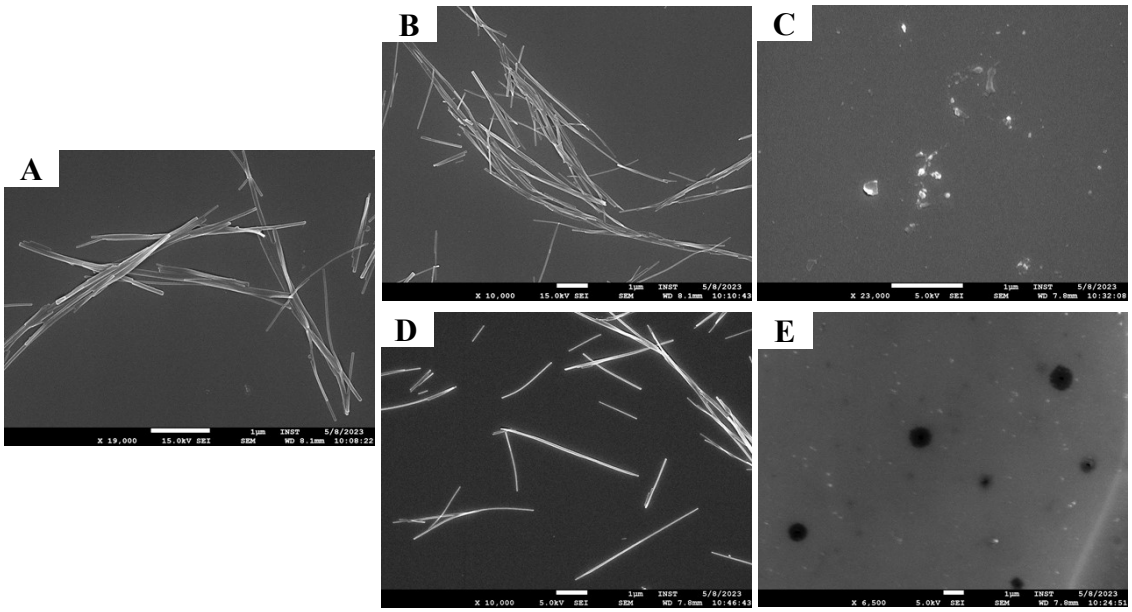

Figure S8. Aβ42 fibrils incubated for 48 h at 37 °C in the presence of amino acid enantiomers, and in the presence or absence of RΔF-SeNPs. (A). Aβ42 fibrils, (B). Aβ42 + D-Ala, (C). Aβ42 + D-Ala+RΔF-SeNPs, (D). Aβ42 + L-Ala, (E). Aβ42 + L-Ala + RΔF-SeNPs. Amyloid fibrils are depicted in the FE-SEM.

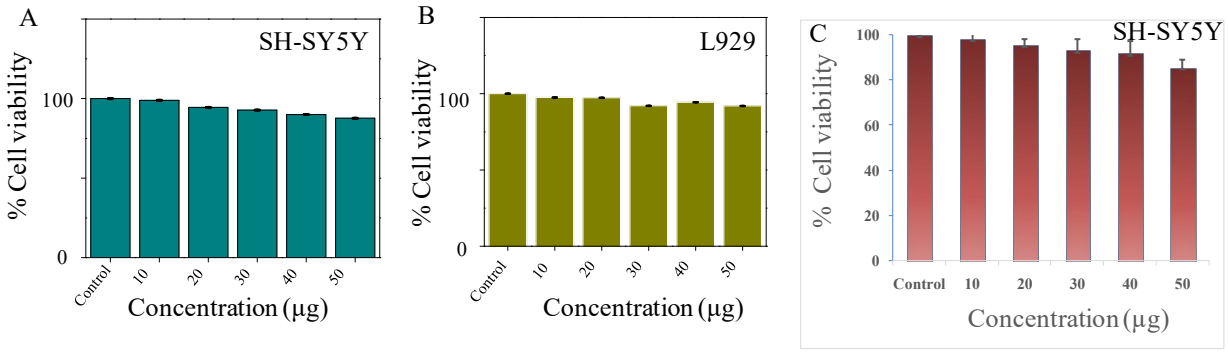

Figure S9. Biocompatibility of RΔF-SeNPs towards (A) SH-SY5Y cells (B) L929, cells analyzed via MTT assay (C) Biocompatibility of RΔF-SeNPs towards SH-SY5Y cells analyzed via resazurin assay.

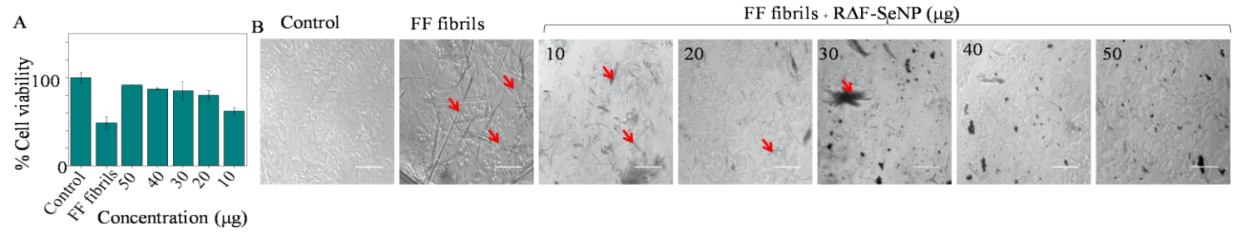

Figure S10. (A) Concentration-dependent protective effects of RΔF-SeNPs exhibited against FF associated cytotoxicity in neuroblastoma, SH-SY5Y cells assessed via MTT assay. (B) Microscopic analysis showing morphology of SH-SY5Y cells co-treated with FF fibrils and the NPs. With increasing concentration of RΔF-SeNPs, cells regained their original structure. (Scale bar 100 µm)

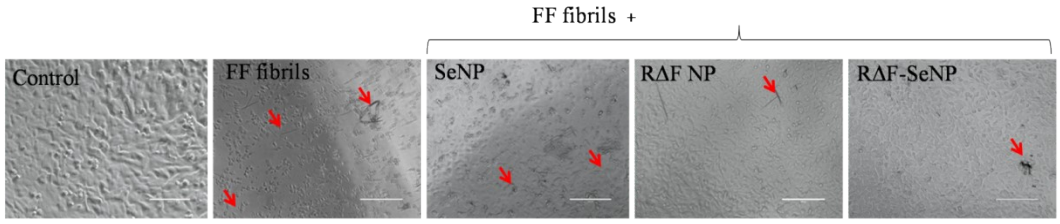

Figure S11. Inverted microscopic images revealing the morphological structure of SH-SY5Y cells. Cells co-incubated with the FF fibrils alone depicted distorted morphology whereas those co-incubated with the RΔF NPs and SeNPs illustrated a change in their morphological structure when compared to the non-treated cells. However, SH-SY5Y cells co-incubated with the fibrils and RΔF-SeNPs revealed morphologies similar to the control cells. Red arrow indicates FF fibrils. (Scale bar 200 µm).

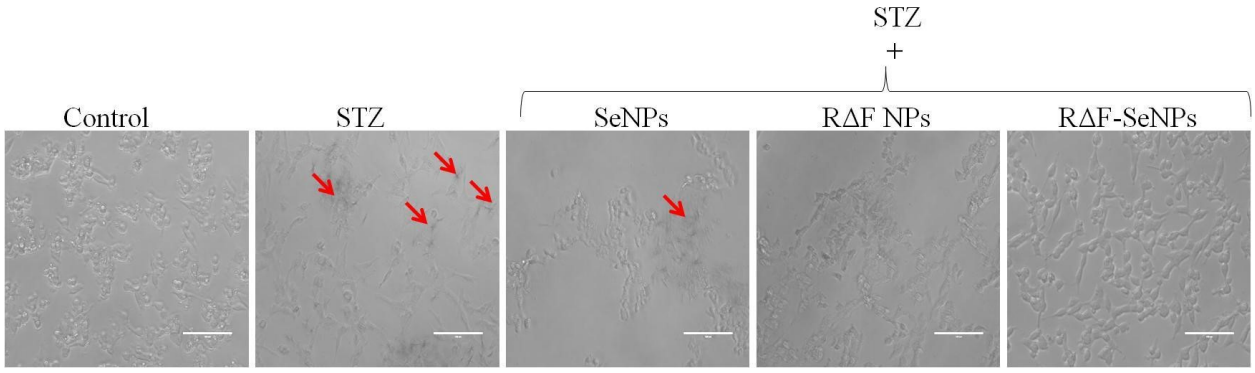

Figure S12. Inverted microscopic images depicting amyloid aggregation in neuronal cells (N2a). Cells treated with STZ, expressed amyloid protein aggregation. The red arrow indicates amyloid aggregation in the cells. SeNPs and bare RΔF NPs co -incubated with cells exerted a protective role in the formation of amyloid aggregates to some extent. Whereas those incubated with RΔF-SeNPs did not exhibit any aggregate formation and morphology of the cells was also found to be normal. (Scale bar 100 μm)

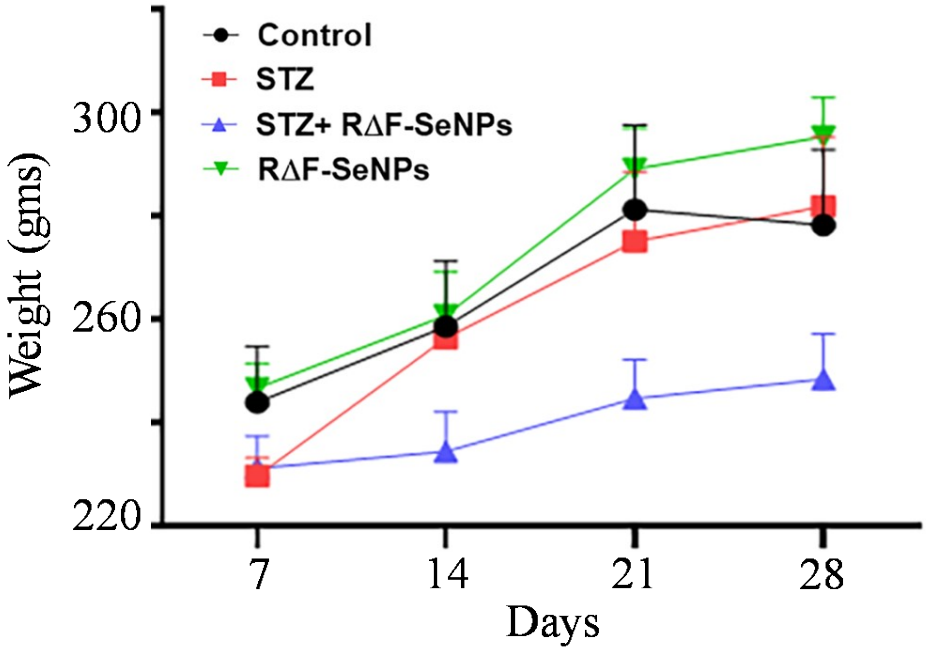

Figure S13. Body weight analysis of rats administered with RΔF-SeNPs in STZ induced animal AD model. No significant change was observed in the body weight of rats treated with STZ+ RΔF-SeNPs, RΔF-SeNPs only with respect to control. A minor change in weight change was observed in case of STZ only with respect to control.

REFERENCES

1 J. J. Panda, A. Kaul, S. Kumar, S. Alam, A. K. Mishra, G. C. Kundu and V. S. Chauhan, *Nanomedicine (Lond)*, 2013, 8, 1927–1942.

2 P. K. Singh, S. Chibh, T. Dube, V. S. Chauhan and J. J. Panda, *Pharm Res*, 2018, 35, 35.

3 A. Kour, T. Dube, A. Kumar and J. J. Panda, *Bioconjugate Chemistry*, 2022, 33, 397–410.

4 J. J. Panda, A. Kaul, S. Kumar, S. Alam, A. K. Mishra, G. C. Kundu and V. S. Chauhan, *Nanomedicine*, 2013, 8, 1927–1942.